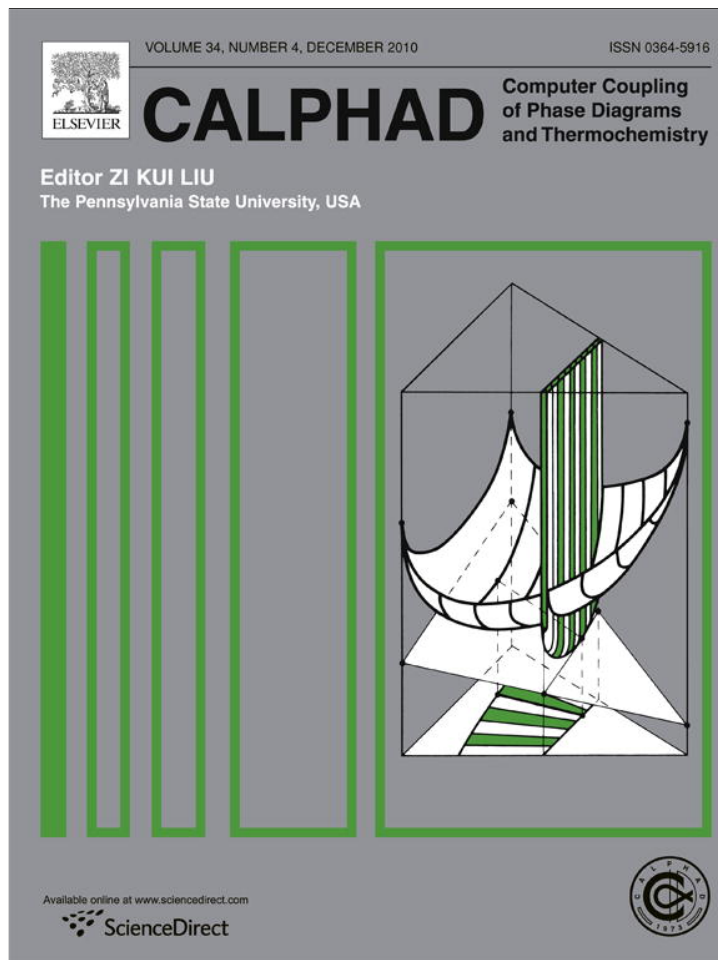


Provided for non-commercial research and education use.
Not for reproduction, distribution or commercial use.



(This is a sample cover image for this issue. The actual cover is not yet available at this time.)

This article appeared in a journal published by Elsevier. The attached copy is furnished to the author for internal non-commercial research and education use, including for instruction at the authors institution and sharing with colleagues.

Other uses, including reproduction and distribution, or selling or licensing copies, or posting to personal, institutional or third party websites are prohibited.

In most cases authors are permitted to post their version of the article (e.g. in Word or Tex form) to their personal website or institutional repository. Authors requiring further information regarding Elsevier's archiving and manuscript policies are encouraged to visit:

<http://www.elsevier.com/copyright>



Contents lists available at ScienceDirect

CALPHAD: Computer Coupling of Phase Diagrams and Thermochemistry

journal homepage: www.elsevier.com/locate/calphad

Relative stability of ordered phases in bcc Cu–Al–Zn

F. Lanzini^{a,*}, R. Romero^a, G.H. Rubiolo^b^a Instituto de Física de Materiales Tandil, Universidad Nacional del Centro de la Provincia de Buenos Aires and Comisión de Investigaciones Científicas de la Provincia de Buenos Aires (CICPBA), Pinto 399, 7000 Tandil, Argentina^b Departamento de Materiales (GIDAT-CAC) CNEA, Instituto Sabato, Universidad Nacional de San Martín, and Consejo Nacional de Investigaciones Científicas y Tecnológicas (CONICET), Avda. Gral. Paz 1499, B1650KNA San Martín, Buenos Aires, Argentina

ARTICLE INFO

Article history:

Received 2 March 2011

Received in revised form

9 May 2011

Accepted 25 May 2011

Available online 16 June 2011

Keywords:

Shape memory alloys

Thermodynamic modelling

Atomic ordering

Cluster Variation Method

Phase diagrams

ABSTRACT

The relative stability of the short range ordered and different long range ordered structures in body centered cubic Cu–Al–Zn is studied by means of the Cluster Variation Method in the Irregular Tetrahedron approximation (IT-CVM). The energetic parameters (constant pair interchange energies for first and second neighbor pairs) used in our calculations have been extracted from experimental order–disorder transition temperatures. It is shown that the use of constant pair interchange energies allows accurate reproduction of the experimental transition temperatures in the binary subsystems Cu–Al and Cu–Zn. Several isothermal sections of the ternary system at temperatures between 600 and 900 K have been calculated. The two–phase field for compositions around Cu₃Al in the ternary system was determined: It was found that such region extends to around 15 at.% Zn in the pseudo–binary Cu_{0.76–0.5x}–Al_{0.24–0.5x}–Zn_x.

© 2011 Elsevier Ltd. All rights reserved.

1. Introduction

The bcc β phase of the ternary Cu–Al–Zn alloy deserves attention due to its various technological applications. Besides the importance of this system in relation to the properties of aluminum brasses, it has an interesting shape memory behavior associated with a martensitic transformation that takes place at low temperatures. This non-diffusive transformation occurs from the disordered or short range ordered bcc (A2) or one of the long range ordered structures derived from it (B2, L2₁, DO₃) to a close packed structure (martensite). Cooling from high temperatures the disordered β phase could suffer one or two ordering reactions; the number and nature of such transitions depend on the alloy composition. The type and degree of order present in the β phase¹ at a given composition and temperature constitutes a very important point in relation to the martensitic transformation: The degree of order in the parent phase is inherited by the martensitic phase, modifying its physical properties. Thus, the study of ordering phenomena in these systems deserves interest not only from the point of view of basic research, but also for their potential technological applications.

* Corresponding author. Tel.: +54 2293 439670; fax: +54 2293 439679.

E-mail address: flanzini@exa.unicen.edu.ar (F. Lanzini).

¹ For the sake of clarity, we will use the term “ β phase” to refer both to the short range ordered bcc phase, A2, and to the long range ordered phases derived from it (B2, L2₁ or DO₃).

In a recent work [1] the temperatures of the ordering transitions for a considerable number of alloys in the line of compositions Cu_{0.76–0.5x}–Al_{0.24–0.5x}–Zn_x have been measured. This line of compositions, joining the binaries Cu_{0.76}Al_{0.24} and Cu_{0.52}Zn_{0.48}, corresponds to a constant conduction electron to atom ratio, $e/a = 1.48$. It has been shown that, for the compositions richer in Al ($x \leq 0.05$), there is a single ordering reaction from the short range disordered configuration, A2, to a state with long range order in nearest and next nearest neighbors L2₁ (DO₃). For higher Zn contents, this transition splits into two separate stages; a first transition from A2 to B2 (CICs type configuration) is followed by a B2 \rightarrow L2₁ transition at lower temperatures. Based on these experimental results, a set of pairwise energetic parameters (interchange energies) has been deduced, which allows an accurate reproduction of the experimental data in that particular pseudo–binary section. The present work can be considered an extension of [1], as it is aimed to explore several questions that arise naturally from the above mentioned results.

A first question refers to the validity of these interchange energies for other compositions beyond those that have been previously studied. In the present work, we analyze the predictions of these interchange energies in the limiting binary alloys Cu–Al, Cu–Zn and Zn–Al, and compare these results with the experimental data available (Section 3.1). The phase competition between the different ordered phases in the ternary Cu–Al–Zn is explored by calculating four isothermal sections, corresponding to $T = 600, 700, 800$ and 900 K (Section 3.2). There is another important issue to be treated in this work: In the binary bcc Cu–Al alloy, at

compositions close to Cu_3Al and temperatures around 800 K, there is a two-phase field between the short range ordered phase A2 and a structure with long range order in first and second neighbors, DO_3 [2]. This two-phase region also should exist in ternary systems based on Cu_3Al with small additions of the third element: In fact, experimental studies in Cu–Al–Mn [3], Cu–Al–Zn [1] and Cu–Al–Be [4–6] reported a first-order character of the ordering reactions in alloys with a low content of the third element, thus indicating the existence of such coexistence region [7]. However, for none of these systems an estimate of the extension of this two-phase field has been given. This is not a minor point, attending to the effects that this possible heterogeneity in the matrix bcc phase may have in the low temperature martensitic transformation. In the present work, we perform a first estimation of the size of the two-phase field in the ternary Cu–Al–Zn system, with particular emphasis in the line of compositions $\text{Cu}_{0.76-0.5x}\text{Al}_{0.24-0.5x}\text{Zn}_x$; these results are presented in Section 3.3.

Several theoretical techniques to study the relative stability of different ordered or disordered phases are available nowadays; a revision of them can be found in [8–10]. Two of these methods have proven to be more useful to determine phase equilibria at finite temperatures [9]: The Cluster Variation Method (CVM), introduced by Kikuchi [11], and the Monte Carlo (MC) simulation method [12,13]. The MC technique has proven to be a very accurate method, provided that a suitable Hamiltonian and the correct energetic parameters are used. The main drawback of this method is that, even with the computational facilities available nowadays, the simulations of some systems are significantly time consuming and, therefore, impractical. For instance, a survey in the literature shows that a comparatively minor number of publications applies the MC method to the study of phase equilibria in ternary alloys, and these studies generally restrict the calculations to a reduced range of compositions. On the other hand, the CVM is a variational method in which the entropy is formulated analytically in terms of the occupation probabilities of a given maximal cluster. This formulation implies a truncation of the configurational entropy, given by the size of the maximal cluster (see, for instance, [14]). The minimizations involved in this method can be performed with much less computational effort than that required by the MC method. In addition, it has been shown that the phase diagrams calculated in binary systems within the so-called irregular tetrahedron (IT) approximation of CVM (Section 2) agree closely with the ones predicted by the MC method [15,16]. Consequently, this approximation has become the preferred tool for the calculation, also, of phase diagrams in ternary bcc systems. In the present work, the phase diagrams of the binary systems Cu–Al, Cu–Zn and Zn–Al, and four isothermal sections of the Cu–Al–Zn phase diagram are calculated within IT-CVM. For some particular range of compositions and temperatures, the predictions of IT-CVM are benchmarked against results of the MC method.

Although, as will be shown below, the present semi-empirical approach satisfactorily reproduces the observed order–disorder transitions in the binary subsystems and a vertical section of the ternary system, there is no reason to rely on the predicted enthalpies of formation of the compounds in the limit of the IT approximation. For example, it is known that the binary ground state diagrams results symmetrical and there is a constraint between the enthalpies of formation for compounds at the equiatomic composition. As has been shown in [17] for the Cu–Al case in particular, a more elaborate approach including multi-body interactions can lead to a drastic change in the morphology of the predicted phase diagram and values of the pairwise energy parameters. But, such an approach goes beyond the IT cluster expansion and to the authors' knowledge there exists no extension in the literature to a ternary system using either CVM or MC calculations. Then, the numerical values of the pairwise energy

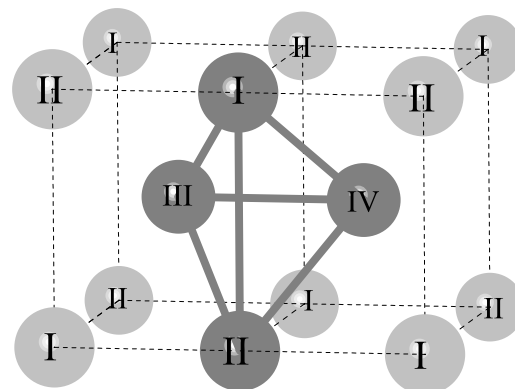


Fig. 1. The irregular tetrahedron cluster in the bcc lattice.

parameters used in this work are to be taken as “effective” interaction energies.

The present paper is organized as follows. In Section 2 we present the methodology implemented for the calculations, i.e., the formalism of the Cluster Variation Method in the irregular tetrahedron approximation, and the minimization procedure utilized. In Section 3 the results of our calculations are presented: The predictions of IT-CVM for the three limiting binaries are discussed in Section 3.1; these results are confronted with experimental data and with MC calculations over reduced ranges of composition and temperatures. In Section 3.2, four ternary Cu–Al–Zn isothermal sections calculated within IT-CVM are presented. These isotherms correspond to $T = 600, 700, 800$ and 900 K. In Section 3.3, a close inspection of the predictions of the method along the pseudo-binary section $\text{Cu}_{0.76-0.5x}\text{Al}_{0.24-0.5x}\text{Zn}_x$ ($\text{Cu}_{0.76}\text{Al}_{0.24} \leftrightarrow \text{Cu}_{0.52}\text{Zn}_{0.48}$) is made. The use of CVM calculations in the grand-canonical ensemble allows an estimation of the extension of the two-phase field at compositions around Cu_3Al . Results for this line of composition are confronted with previous results of MC simulations in the canonical ensemble. Finally, in Section 4 we discuss the results and outline the conclusions.

2. Methodology

The Cluster Variation Method (CVM) is the name of a hierarchy of approximations to the configurational free energy of an alloy. This method was firstly proposed by Kikuchi [11] and has been extensively applied to the study of different alloy systems. The main idea behind the CVM is to write the configurational free energy of the alloy as a function of the probabilities of occupation of a given maximal cluster; as the number of atoms contained in this maximal cluster increases, so does the accuracy of the approach. For bcc based binary alloys, it has been shown that sufficiently accurate results [15,16] can be reached by using, as a maximal cluster, an irregular tetrahedron as the one shown in Fig. 1.

The irregular tetrahedron comprehends four first neighbor pairs (I–III, I–IV, II–III and II–IV) and two second neighbor pairs (I–II and II–IV). If Z_{ijkl} represents the probability that atoms of types i, j, k , and l (for a binary alloy, i, j, k, l can take one between two values – 0 and 1, for instance – representing the two type of atoms; for a ternary system, they take one between three different values) occupy the sites I to IV (in this order), then the configurational grand potential of the system:

$$\Omega = U - T \cdot S - N \sum_{i=1}^n \mu_i \cdot x_i \quad (1)$$

can be written in terms of the cluster probabilities Z_{ijkl} . The configurational internal energy, U , and the configurational entropy, S ,

take the form [18]:

$$U = 6N \sum_{ijkl} \varepsilon_{ijkl} Z_{ijkl} \quad (2)$$

$$S = -Nk_B \left\{ 6 \sum_{i,j,k,l} L(Z_{ijkl}) - 3 \sum_{i,j,k} (L(U_{ijk}^{I-II-III}) + L(U_{ijk}^{I-II-IV})) \right. \\ + L(U_{ijk}^{I-III-IV}) + L(U_{ijk}^{II-III-IV}) \\ + \frac{3}{2} \sum_{i,j} (L(V_{ij}^{I-II}) + L(V_{ij}^{III-IV})) + \sum_{i,j} (L(Y_{ij}^{I-III}) \\ + L(Y_{ij}^{I-IV}) + L(Y_{ij}^{II-III}) + L(Y_{ij}^{II-IV})) \\ \left. - \frac{1}{4} \sum_i (L(p_i^I) + L(p_i^{II}) + L(p_i^{III}) + L(p_i^{IV})) \right\} \quad (3)$$

with k_B the Boltzmann constant and $L(x) = x \cdot \ln(x)$. In the preceding expressions, ε_{ijkl} is the energy of a tetrahedron with occupation i, j, k, l . The remaining probabilities appearing in the entropy expression ($U_{ijk}^{\alpha-\beta-\gamma}$, $V_{ij}^{\alpha-\beta}$, $Y_{ij}^{\alpha-\beta}$ and p_i^α) refer to the probability of occupation of sub-clusters embodied in the tetrahedron (triangles, first neighbor pairs, second neighbor pairs and sites, respectively), and are just linear combinations of the Z_{ijkl} 's. These relations (reduction relations), can be found in Refs. [16,19]. The last term in Eq. (1) contains the atomic fractions of each element, x_i , which are related to the site probabilities by means of

$$x_i = \frac{1}{4} (p_i^I + p_i^{II} + p_i^{III} + p_i^{IV}). \quad (4)$$

The chemical potentials μ_i are not all independent, and it is possible to introduce a new set of chemical potentials μ_i^* (the “baricentric” chemical potentials, [19,20]) which fulfill the relation

$$\sum_i \mu_i^* = 0.$$

For an n -components alloy, this condition is achieved by defining [19]

$$\mu_i^* = \mu_i - \frac{1}{n} \sum_{j=1}^n \mu_j.$$

With this transformation, the equilibrium state of an alloy at a given temperature T and “baricentric” chemical potentials $\{\mu_i^*\}$ is found by minimizing the CVM potential

$$\Omega^* = U - T \cdot S - N \sum_{i=1}^n \mu_i^* \cdot x_i \quad (5)$$

with respect to the cluster probabilities Z_{ijkl} . It is worth emphasizing that the molar fractions of the different elements, x_i , are not fixed a priori but obtained as a by-product of the minimization.

There are two different methods that can be used to minimize the CVM potential in Eq. (5): The Newton–Raphson method and the natural iteration method (NIM) developed by Kikuchi [21]. In the present work we have chosen the latter; a clear description of the iteration mechanism involved in NIM can be found in [18].

When the energetics of a given alloy system being restricted to the consideration of pair interactions alone (i.e., neglecting multi-body corrections), the ordering or clustering tendency of different atomic species is better described by the so-called interchange energies $W_{AB}^{(k)}$, defined as:

$$W_{AB}^{(k)} = -2V_{AB}^{(k)} + V_{AA}^{(k)} + V_{BB}^{(k)}$$

with $V_{AB}^{(k)}$ the interaction potential between atoms of specie A and B placed at the distance corresponding to k -th neighbors (please note that the linear combination above differs by a factor 2, and a sign inversion, with the expression used by other authors, e.g. Ref. [19]).

Table 1

First and second neighbors interchange energies for the Cu–Al–Zn system [1] ($1k_B K = 8.31 J/mol$).

$W_{CuZn}^{(1)} = 955k_B K$	$W_{CuZn}^{(2)} = 535k_B K$
$W_{CuAl}^{(1)} = 1660k_B K$	$W_{CuAl}^{(2)} = 920k_B K$
$W_{ZnAl}^{(1)} = -45k_B K$	$W_{ZnAl}^{(2)} = 285k_B K$

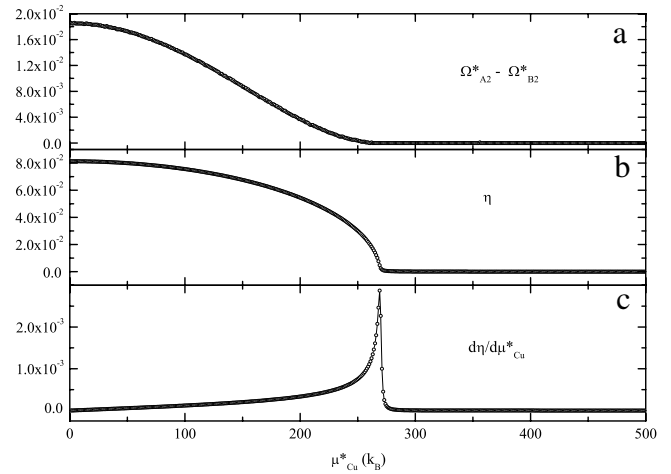


Fig. 2. Continuous A2 ↔ B2 transition in Cu–Al at 1300 K. (a) Difference in the CVM potential of both phases. (b) Evolution of the Iro parameter η . (c) Derivative of η respect to the chemical potential; the peak in this curve is identified as the transition point.

In Ref [1], a set of constant interchange energies for first and second neighbor pairs for bcc Cu–Al–Zn has been determined (Table 1). These values have been derived by fitting to the measured order–disorder temperatures along the line of compositions $Cu_{0.76-0.5x}Al_{0.24-0.5x}Zn_x$ by performing Monte Carlo simulations in the canonical ensemble.

The cluster energies ε_{ijkl} in Eq. (2) can be written as linear combinations of the interchange energies:

$$\varepsilon_{ijkl} = -\frac{1}{12} (W_{ik}^{(1)} + W_{il}^{(1)} + W_{jk}^{(1)} + W_{jl}^{(1)}) - \frac{1}{8} (W_{ij}^{(2)} + W_{kl}^{(2)}). \quad (6)$$

In this work, we take as a starting point the interchange energies listed in Table 1. By replacing these interchange energies into the CVM potential (Eq. (5)) through (Eq. (6)) and performing its minimization with NIM, the phase diagram of the ternary bcc Cu–Al–Zn system (and of the three limiting binaries) has been calculated. In order to determine the point at which a given phase transition takes place, we have used different criteria according to the nature of the phase transition is first-order or continuous. In the first case, the values of the chemical potentials $\{\mu_i^*\}$ at which the transition takes place is determined by evaluating the CVM potentials (5) for the two competing phases, and determining the point where they intersect. For continuous (second order) transitions the problem of determining the point at which the transition occurs has to be considered with some more detail. The second order transition point can be determined by calculating the second Hessian determinant, or by plotting the difference in grand potentials between both phases against chemical potential and searching for the point where this difference vanishes [18]. The drawback of the second procedure is that the grand potentials of both phases do not really intersect, but they contact at the transition point with the same slope; the convergence between the curves is generally so fuzzy that a determination of the intersection point can be difficult (Fig. 2(a)). In the present work, we used an alternative approach that yields equivalent results, and it is based on the fact that the ordered phase has no metastable continuation

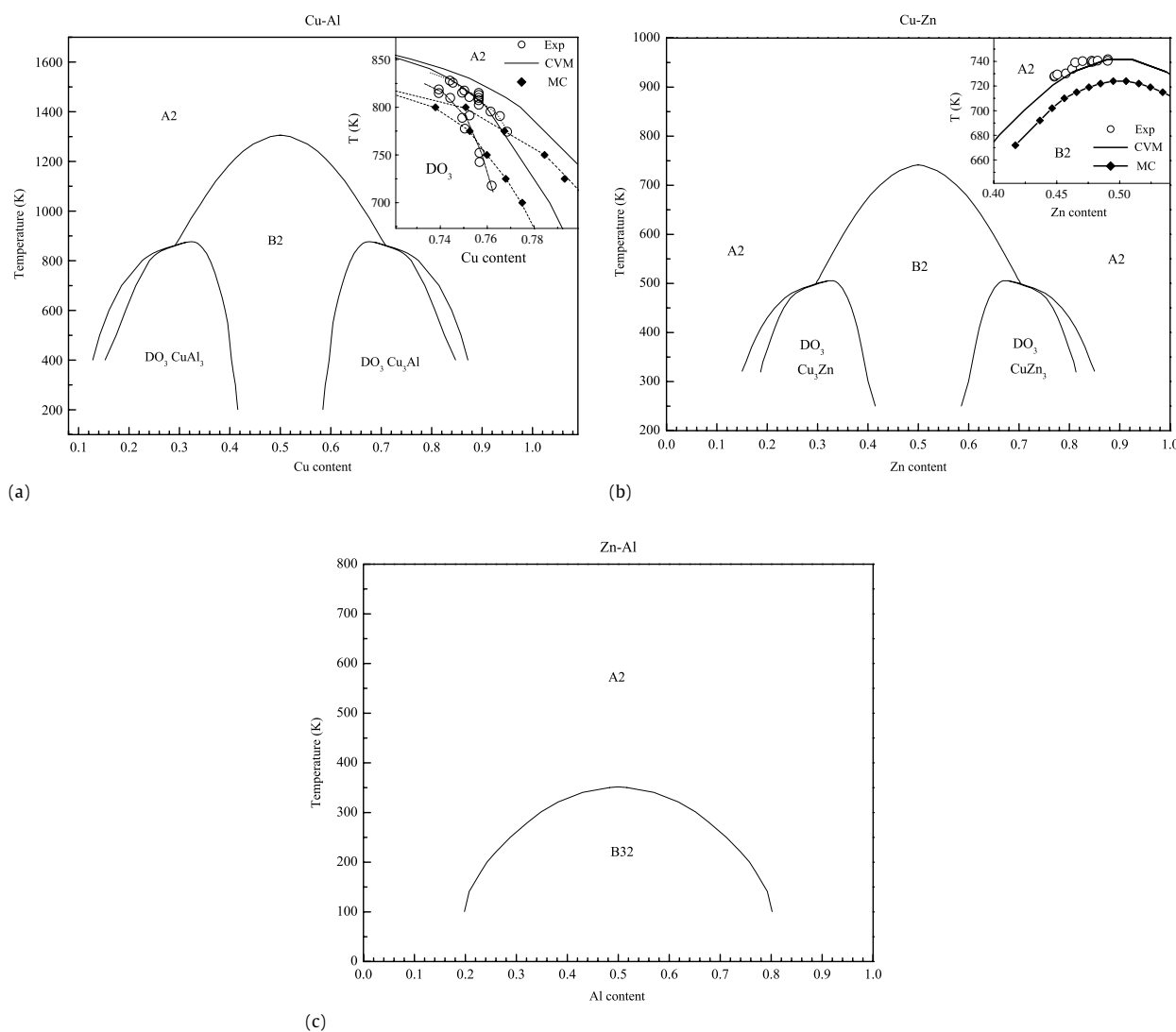


Fig. 3. Calculated phase diagrams for (a) Cu–Al, (b) Cu–Zn and (c) Zn–Al. The insets show the comparison with experimental measurements [2,25].

in the range of stable disordered states. For each second order transition, we defined an order parameter η representative of the Iro degree in the ordered phase (or, strictly speaking, in the less symmetrical phase). This order parameter can be constructed as a difference between site occupation probabilities, p_i^α . Starting from the ordered state and varying the chemical potential this order parameter gradually vanishes (Fig. 2(b)). We have taken as the point of the second order transition the one at which $\frac{\partial \eta}{\partial \mu^*}$ shows a peak (Fig. 2(c)). This situation is illustrated in Fig. 2 for the A2 \leftrightarrow B2 transition in the binary Cu–Al at 1300 K. For this transition, the long range order parameter can be defined as the difference between Cu occupation of sublattices I and II: $\eta \propto p_{CuI}^I - p_{CuI}^{II}$. The same criterion has been used for the ternary system and for other kind of continuous transitions (with a proper definition of η). It should be noted, however, that a naive use of derivatives to locate transitions could lead to the detection of “spurious” miscibility gaps close to stoichiometric compositions at low temperatures [22–24].

3. Results

3.1. Binary subsystems

The predicted phase diagrams for the binary systems Cu–Al, Cu–Zn and Zn–Al are represented in Fig. 3(a)–(c), respectively.

The insets in Fig. 3(a)–(b) indicate that the pair interchange energies in Table 1 reasonably reproduce the measured order–disorder transitions in both Cu–Al and Cu–Zn (in the range of compositions in which the bcc structure is stable or can be retained in metastable form). The inset in Fig. 3(a) shows a reduced range of compositions around the stoichiometric Cu_3Al . The circles correspond to the limits of the A2/ DO_3 two-phase field according to the data compiled by Murray [2]. Despite our CVM calculations slightly overestimating the temperatures of such limits, the agreement with the experiment can be considered satisfactory. As discussed above, the truncation of the entropic term in CVM leads to some overestimation of the transition temperatures in comparison with the MC results that are, in principle, exacts. In order to estimate the degree of inaccuracy, we benchmarked both methods in the reduced range of compositions and temperatures shown in the inset of Fig. 3(a). It can be seen that both methods agree with the topology of the two-phase region. The temperatures of the A2/A2 + DO_3 and A2 + DO_3 / DO_3 limits predicted by IT-CVM are roughly 5% above the MC predictions; other authors [15,16] had found a similar deviation. A similar comparison for the A2 \leftrightarrow B2 continuous transition in bcc Cu–Zn is made in the inset of Fig. 3(b). Again, the predictions of IT-CVM are in reasonable agreement with the MC results. The fact that, in this case, the transition temperatures calculated with CVM reproduce more closely the experimental data [25] indicates

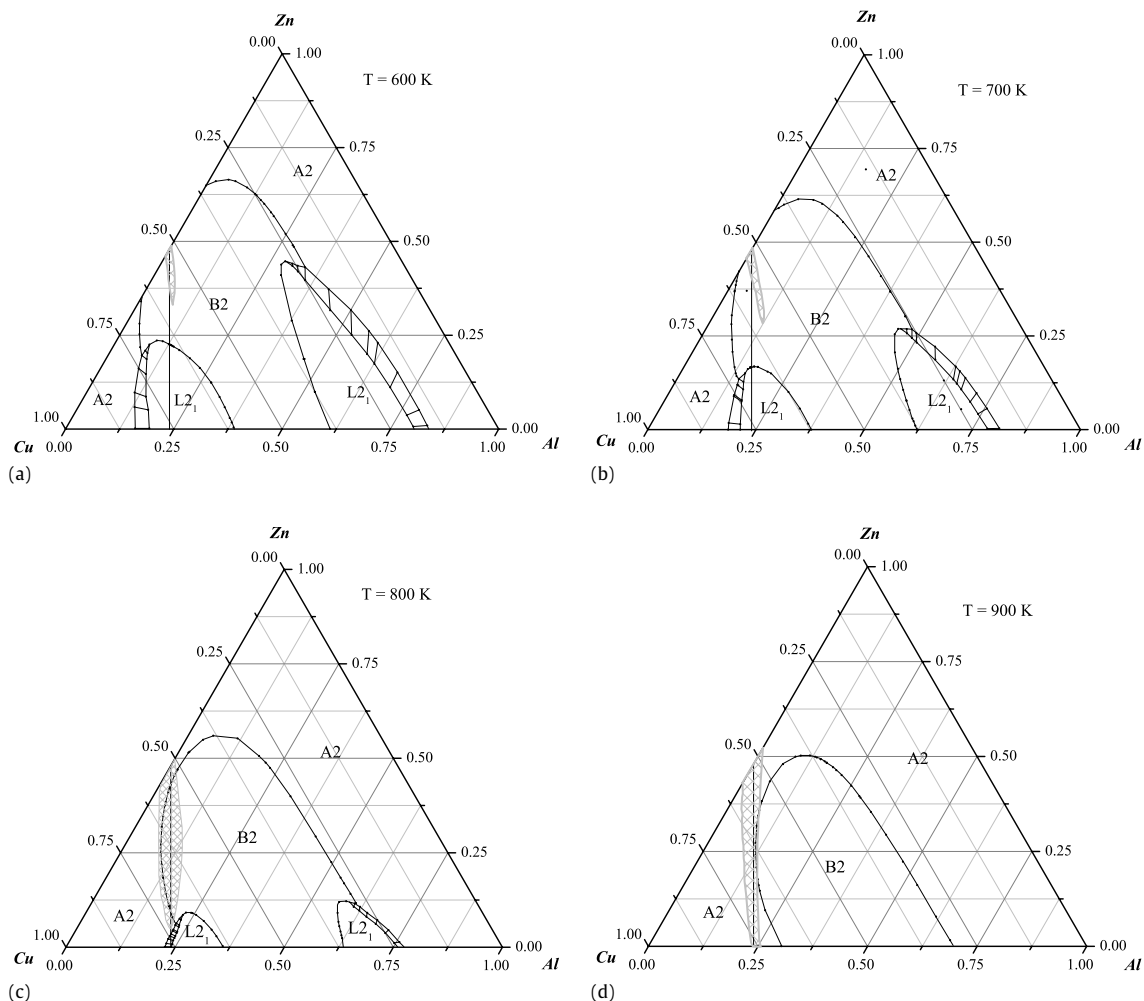


Fig. 4. Calculated isothermal sections in the Cu–Al–Zn system. The straight line represents the set of compositions $\text{Cu}_{0.76-0.5x}\text{-Zn}_x\text{-Al}_{0.24-0.5x}$, and the grey shaded regions are the stability limits of the bcc based structures.

that the values of $W_{\text{CuZn}}^{(1)}$ and $W_{\text{CuZn}}^{(2)}$ are somewhat below their actual values. In general, despite these minor discrepancies with respect to the experimental temperatures of the transitions, the phase stability limits are satisfactorily reproduced by our model. Both the nature of the transitions (first order or continuous) and that of the involved phases are correctly predicted, and also the morphology of the calculated phase diagram closely follows the experimental data. For the Cu–Al and Cu–Zn systems we performed additional very careful calculations around a Cu content of 0.3 (0.7); these calculations (not shown here) indicate that the narrow two-phase fringe extends up to near the top of the DO_3 field, and, then, that the phase rules are not violated.

The predictions for the Zn–Al system cannot be confronted with experimental information, because this system does not display a bcc structure in any range of compositions [26]. However, the fact that our calculations only predict a hypothetical ordered phase at low temperatures (Fig. 3(c)) is consistent with the fact that Zn and Al atoms do not show ordering tendency.

3.2. Ternary isothermal sections

In Fig. 4(a)–(d), four complete isothermal sections of the ternary Cu–Al–Zn phase diagram are represented.

The straight line represents the compositions with a conduction electron to atom ratio $e/a = 1.48$, that will be discussed with more detail in Section 3.3. The phase diagrams are dominated by

the existence of a wide region of stability of the B2 structure. This region centers on the line connecting the two stoichiometric binaries CuAl and CuZn. As the temperature increases the B2 field stretches, keeping the same topology. At 600, 700 and 800 K, the L2_1 phase, ordered in first and second neighbors is stable within composition ranges centered on Cu_3Al and CuAl_3 , respectively. Superimposed onto our calculations, we have drawn the (approximated) regions of stability of the bcc structure [27]. Although we present, for the sake of completeness, the full isothermal sections, the range of compositions that deserves attention from the point of view of practical applications is the grey-shaded region and their immediate surroundings. At compositions well apart from this region the bcc structure (and the ordered structures derived from it) is not stable, nor can it be retained in metastable form.

A word of caution with respect to the nature of the phase ordered in first and second neighbors is necessary at this point: We have not made a clear distinction between DO_3 and L2_1 structures yet. The first name, DO_3 , is generally reserved to binary alloys, whereas in ternary systems both structures have been reported. A binary stoichiometric DO_3 compound (prototype Fe_3Al) has composition A_3B , and its atomic distribution can be seen with the help of Fig. 1, by imagining the A atoms occupying sites I, II and III, and B atoms in sites IV. A ternary stoichiometric L2_1 compound has composition A_2BC (prototype Cu_2AlMn), with A atoms on sites I and II, B atoms on IV and C atoms on III. Both structures are symmetrically equivalent [28] and, consequently,

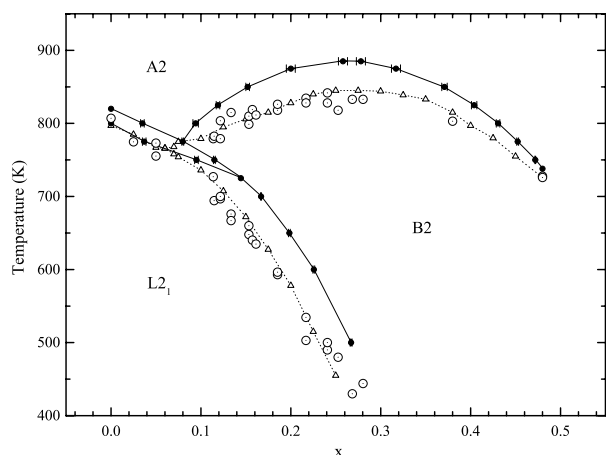


Fig. 5. Transition temperatures for alloys along the line of compositions $\text{Cu}_{0.76-0.5x}\text{-Al}_{0.24-0.5x}\text{-Zn}_x$. Open circles are the experimental results, and the triangles represent the fitting with MC simulations [1]. The black circles are the corresponding IT-CVM results.

some publications do not make a clear distinction between them. In the off-stoichiometric case, the two structures are better distinguished in terms of the site occupation probabilities, p_i^{α} . For the DO_3 configuration, $p_A^{\text{I}} = p_A^{\text{II}} = p_A^{\text{III}} \neq p_A^{\text{IV}}$, whereas for L2_1 order $p_A^{\text{I}} = p_A^{\text{II}} \neq p_A^{\text{III}} \neq p_A^{\text{IV}}$ [29]. In the present calculations, the phase ordered in first and second neighbors has, both in the binary and the ternary cases, site occupation probabilities that correspond to the definition given above for L2_1 order (except, probably, at very low temperatures and compositions close to the stoichiometry A_3B). However, in the binary phase diagrams of Fig. 3, we have conserved the historical convention. In fact, if the atomic distribution were the one strictly corresponding to the site occupation probabilities of a DO_3 structure, the transition from the B2 phase would have to be first-order, as imposed by the symmetry of the involved phases [3]; as can be seen in Fig. 3(a)–(b), this is not the case.

3.3. Section $\text{Cu}_{0.76-0.5x}\text{-Zn}_x\text{-Al}_{0.24-0.5x}$

In Fig. 5 the measured order-order and order-disorder temperatures for alloys with compositions along the line $\text{Cu}_{0.76-0.5x}\text{-Al}_{0.24-0.5x}\text{-Zn}_x$ ($e/a = 1.48$) are represented with open circles. The triangles represent the fit to the experimental data with MC simulations in the canonical ensemble [1], using the same set of interchange energies as in the present work (Table 1). The black circles in Fig. 5 represent the predictions of IT-CVM in the grand canonical ensemble. Critical temperatures have been determined by calculating the intersection of the phase frontiers in different isothermal sections with the straight line representing the compositions of interest, as indicated in Fig. 4; the uncertainties in composition associated with this procedure are represented as horizontal bars.

The major aim for the re-assessment in this line of compositions was to make an estimation of the extent of the two-phase field in the ternary system. As discussed in the Introduction, this is a question that deserves attention from the point of view of practical applications. The coexistence region is wedge-shaped, with a maximum broadening in temperatures around 20 K in the binary edge $x = 0$ and becoming gradually thinner as the Zn content increases. The gap closes at around 15 at.% Zn. For low Zn contents the coexisting phases are A2 and L2_1 (DO_3), whereas for higher contents of Zn and temperatures below 775 K the coexisting phases are B2 and L2_1 . It is worth noting that calorimetric measurements on alloys with Zn contents up to $x = 0.05$ show that the peak associated with the ordering reaction has the typical shape of a

first-order transition [1], whereas for $x \geq 0.11$ the calorimetric peak of the $\text{B2} \leftrightarrow \text{L2}_1$ transition resembles, more likely, a continuous transition. This seems to indicate that the present calculation slightly overestimates the extent in composition of the two-phase region; however, more detailed information is necessary in order to make a conclusive assertion about this point.

A result of the present calculations is that, as can be seen in Fig. 5, although the IT-CVM correctly reproduces the topology of the phase diagram for this pseudo-binary section, the overestimation of the transition temperatures is considerably greater than the values that have been reported for binary alloys [15,16]. This is an important observation, because there is a considerable number of publications in which ternary phase diagrams are calculated within this approximation, based on the fact that the discrepancies in the binary case are not substantial. However, we have not found a systematic comparison of MC and IT-CVM results for the case of bcc ternary systems. In fact, as the present results show, the differences between MC and IT-CVM transition temperatures at the two binary extremes $x = 0$ and $x = 0.48$ remain between reasonable limits, but they increase as we move away from these compositions and the ternary character of the alloys becomes more relevant. The major discrepancies in Fig. 5 occur at compositions around $x = 0.25$, i.e., well inside the ternary triangle. Given that first and second nearest-neighbor interactions remain the same in the MC and CVM calculations, the accuracy of the free energy determination with the CVM method in the ternary alloy could be improved including higher order correlation functions in the configurational entropy by increasing the size of the maximal cluster [30]. For bcc systems, one appropriate extension could be the octahedron or octahedron-pentuplet maximal cluster [17].

4. Conclusions

In the present work, we analyze the relative stabilities of the different ordered and disordered bcc-based structures in the Cu–Al–Zn systems. Calculations were based on a simple approach involving pair interactions in first and second neighbors, without considering more distant interactions or multi body corrections. The energetic parameters have been extracted from a previous fit to experimental order/disorder temperatures. Determination of the equilibrium state of the alloy at given temperature and chemical potentials has been performed by minimization of the thermodynamic potential obtained in the Irregular Tetrahedron approximation of the Cluster Variation Method (IT-CVM). This approach satisfactorily accounts for the measured order/disorder transitions in the binary Cu–Zn and Cu–Al alloys, and yields transition temperatures that are in agreement with the predictions of the Monte Carlo (MC) method. Four complete isothermal sections of the ternary system at $T = 600, 700, 800$ and 900 K have been calculated using IT-CVM in the grand canonical ensemble. In this range of temperatures, the ternary phase diagram is dominated by a B2 stability field, oriented along the line joining the equiatomic CuZn and CuAl. At $T = 600, 700$ and 800 K, two regions of stability of the L2_1 phase appear, centered at Cu_3Al and CuAl_3 , respectively. A detailed analysis of the pseudo-binary section $\text{Cu}_{0.76-0.5x}\text{-Al}_{0.24-0.5x}\text{-Zn}_x$ indicates the existence of a two-phase field between the short range ordered bcc phase A2 and the low temperature long range ordered phases L2_1 and B2 . This heterogeneous region extends from the binary $\text{Cu}_{0.76}\text{Al}_{0.24}$ and closes at a composition near $\text{Cu}_{0.685}\text{Zn}_{0.15}\text{Al}_{0.165}$.

Acknowledgments

This work was supported by the Agencia Nacional de Promoción Científica y Tecnológica, Consejo Nacional de Investigaciones

Científicas y Técnicas, Comisión de Investigaciones Científicas de la Provincia de Buenos Aires, and Secretaría de Ciencia Arte y Técnica of the Universidad Nacional del Centro. F. L. acknowledges partial support by a CONICET postdoctoral fellowship.

References

- [1] F. Lanzini, R. Romero, M. Stipcich, M.L. Castro, *Phys. Rev. B* 77 (2008) 134207/1–8.
- [2] J.L. Murray, *Int. Met. Rev.* 30 (1985) 211–234.
- [3] E. Obradó, C. Frontera, Ll. Mañosa, A. Planes, *Phys. Rev. B* 58 (1998) 14245–14255.
- [4] M. Jurado, T. Castán, Ll. Mañosa, A. Planes, J. Bassas, X. Alcobé, M. Morin, *Phil. Mag. A* 75 (1997) 1237–1250.
- [5] F. Lanzini, R. Romero, M.L. Castro, *Intermetallics* 16 (2008) 1090–1094.
- [6] M.L. Castro, R. Romero, *Scripta Mater.* 42 (2000) 157–161.
- [7] D.A. Porter, K.E. Easterling, *Phase Transformations in Metals and Alloys*, Taylor and Francis, USA, 1992.
- [8] F. Ducastelle, *Order and Phase Stability in Alloys*, North-Holland, Amsterdam, 1991.
- [9] G. Inden, W. Pitsch, in: P. Haasen (Ed.), *Materials Science and Technology: A Comprehensive Treatment*, in: *Phase Transformations in Materials*, vol. 5, VCH, Weinheim, 1991.
- [10] W. Pfeiler (Ed.), *Alloy Physics. A Comprehensive Reference*, Wiley-VCH, Weinheim, 2007.
- [11] R. Kikuchi, *Phys. Rev.* 81 (1951) 988–1003.
- [12] K. Binder (Ed.), *Monte Carlo Methods in Statistical Physics*, Springer-Verlag, Berlin, 1987.
- [13] O.G. Mouritsen, *Computer Studies of Phase Transitions and Critical Phenomena*, Springer-Verlag, Berlin, 1984.
- [14] T. Mohri, in: W. Pfeiler (Ed.), *Alloy Physics. A Comprehensive Reference*, Wiley-VCH, Weinheim, 2007.
- [15] B. Dünweg, K. Binder, *Phys. Rev. B* 36 (1987) 6935–6952.
- [16] H. Ackermann, G. Inden, R. Kikuchi, *Acta Metall.* 37 (1989) 1–7.
- [17] F. Lanzini, P.H. Gargano, P.R. Alonso, G.H. Rubiolo, *Modelling Simul. Mater. Sci. Eng.* 19 (2011) 015008/1–15.
- [18] C. Colinet, G. Inden, R. Kikuchi, *Acta Metall. Mater.* 41 (1993) 1109–1118.
- [19] L. Eleno, J. Balun, G. Inden, C. Schön, *Intermetallics* 15 (2007) 1248–1256.
- [20] G. Inden, C. Schön, *CALPHAD* 32 (2008) 661–668.
- [21] R. Kikuchi, *J. Chem. Phys.* 60 (1974) 1071–1080.
- [22] M. Sluiter, Y. Kawazoe, *Phys. Rev. B* 59 (1999) 3280–3282.
- [23] A. Kusoffsky, B. Sundman, *J. Phys. Chem. Solids* 59 (1998) 1549–1553.
- [24] C.G. Schön, G. Inden, *Acta Mater.* 46 (1998) 4219–4231.
- [25] P.K. Kumar, L. Muldower, *Phys. Rev. B* 14 (1976) 1972.
- [26] *ASM Metals Handbook*, 8th.ed., vol. 8, Metals Park, Ohio, 1973.
- [27] *Landolt-Börnstein-Group IV Physical Chemistry, Numerical Data and Functional Relationships in Science and Technology, Light Metal Systems. Part 2: Selected Systems from Al–Cu–Fe to Al–Fe–Ti*, vol. 11A2, Springer, Berlin, Heidelberg, 2005.
- [28] G.Y. Guo, G.A. Botton, Y. Nishino, *J. Phys.: Condens. Matter* 10 (1998) L119–L126.
- [29] M. Ahlers, *Prog. Mater. Sci.* 30 (1986) 135–186.
- [30] P.D. Tevesch, M. Asta, G. Ceder, *Modelling Simul. Mater. Sci. Eng.* 6 (1998) 787–797.